THERMAL PROTECTION SOLUTION FOR SOLID FUEL ROCKET ENGINES

UDC:621.453A457
Original scientific paper https://doi.org/10.46793/adeletters.2023.2.3.3

Nguyen Minh Phu[1], Vo Van Bien[1*], Nguyen Thanh Hai[1]

[1]The Faculty of Special Equipments, Le Quy Don Technical University, Hanoi City, 100000, Vietnam

Abstract:
This paper presents a new approach to the thermal protection of solid-fuel rocket engines. The method of thermal protection using coatings not only reduces the risk of damage to the engine casing but also increases the engine's efficiency in working. Parameters such as thrust and the mass per square meter of the engine casing are used to compare the differences between engines with and without thermal protection coating. Numerical calculation applied to the cruise engine of the rocket 9M39. Calculation results show that the thickness of the thermal protective coating and the thickness of the combustion chamber have been optimized regarding rocket weight. The survey results showed that the mass per square meter of the engine casing decreased by 2.5 times, and the engine's impulse total increased by 1.13% when using the thermal protective coating. These results are used as data to develop methods to improve the performance of solid propellant rocket engines.

ARTICLE HISTORY
Received: 20 June 2023
Revised: 1 September 2023
Accepted: 19 September 2023
Published: 30 September 2023

KEYWORDS
Thermal protection, thickness of coating, solid propellant rocket engine, rocket engine

1. INTRODUCTION

A solid propellant rocket engine is a thermal machine that converts the chemical energy of propellant into the heat energy of a combustion product [1,2], see in Fig. 1. With a high combustion chamber temperature, the gas flow is ejected through the nozzle; the thrust is created to make the rocket move.

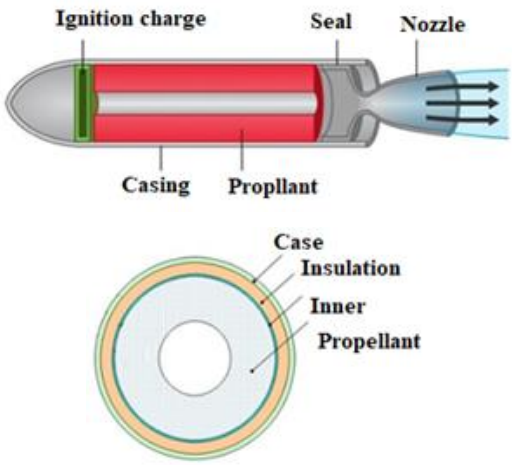

Fig. 1. Solid-fuel rocket engine

The propellant is burned during engine operation, creating a high-temperature gas flow. The temperature of the combustion product is transferred to the surfaces of the engine casing through convection and radiation. This heat transfer causes energy loss in combustion products, reducing the engine's efficiency. In addition, this very high temperature (about 2000 to 2800 K) can destroy the rocket engine casing in a short time. So, calculating the thermal protective coating is very important to work in the design of rocket engines.

In the world, there are many studies on the heat transfer process through the engine wall. These studies mainly focus on finding methods of thermal protection against damage to the engine casing [1-4]. Document [5,6] deals specifically with the issues of chemistry and technologies of resin mixtures fabrication for the internal heat-protective rocket solid fuel engine. However, some research papers on thermal protection materials for rocket engines only provide a method of material selection without providing an optimal solution when used on a solid-fuel rocket engine [7,8]. Numerous studies have mentioned methods of determining defects for thermal protective coatings, studying materials

*CONTACT: V.V. Bien, e-mail: vovanbien@lqdtu.edu.vn

used to make thermal protective coatings [9-12]. In addition, many studies are using the simulation method of heat transfer through the engine wall (CFD) to determine the heat resistance of the engine case when working [13-15]. Previous studies have generally mentioned thermal protection measures for rocket engine cases. However, the detailed evaluation or coordination of methods to protect the engine heat has not been mentioned.

In this paper, the author mentions a thermal protection method for solid-fuel rocket engines using optimal thermal protective coatings. With this coating, the motor wall is not destroyed and, at the same time, ensures the most negligible thickness, reducing the engine's weight when working. In addition, the relationship between the thickness of the motor case and the thermal protection layer is also established in this paper.

2. MATERIALS AND METHODS

The content of the article focuses on establishing a system of interior ballistic equations that consider heat loss. This equation is solved simultaneously with the system of equations for heat transfer through the combustion chamber wall to determine the amount of heat lost when the engine works. In addition, the paper also provides an equation to determine the relationship between the combustion chamber wall thickness and the thickness of the thermal protection layer. Numerical methods are used to solve this system of equations. The calculation program is programmed on MATLAB software. The calculation results are used as data to develop methods to improve the performance of solid propellant rocket engines.

3. ESTABLISHING THE COMPUTATIONAL MODEL

3.1 Heat loss through the combustion chamber wall

The process of heat loss through the wall of the combustion chamber takes place through three stages as follows: Heat transfer from the combustion gas to the inner wall of the combustion chamber; Heat conduction from the inner wall to the outer wall of the combustion chamber and the heat transfer from the outer wall of the combustion chamber to the environment. When there is a thermal protective coating, the heat conduction must pass through two layers (the thermal protector and the combustion chamber wall) before transferring heat to the environment.

To establish the thermal loss calculation model, some assumptions are used as follows:

- Consider the casing of the combustion chamber as a round tube;
- The heat flow through the combustion chamber wall is isotropic;
- The contact surface temperature between the thermal protective coating and the inner surface of the combustion chamber is considered to be the same;
- The coating is considered to be of uniform thickness in all directions and does not change during engine operation.

The calculation model of thermal protective coating consists of 2 layers, see Fig. 2:

- The first layer: Thermal protective coating with thickness $\Delta K = \Delta r$ in direct contact with combustible gas, with an inner surface temperature of coating T_1, and thermal conductivity coefficient is λ_1.
- The second layer: The combustion chamber casing has a thickness of $\Delta P = R - r - \Delta r$, and its inner surface temperature is equal to the outer surface temperature of the coating T_2, and the thermal conductivity coefficient is λ_2.

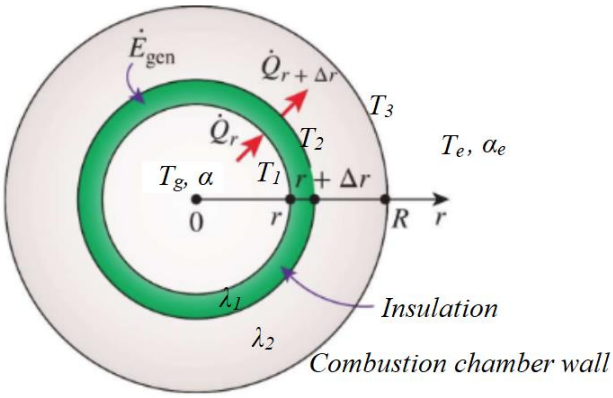

Fig. 2. Thermal protective coating calculation model

3.1.1 Heat transfer of combustible gas to the inner wall of the combustion chamber

The transfer and conduction of heat from the combustion gas to the engine walls is a very complex process. To simplify the calculation process, we can think of the heat transfer process as consisting of only two processes: Convection heat transfer and radiant heat transfer. The process of transferring heat from a high-speed gas stream to the engine wall is represented by the following equation:

$$q_l = \alpha(T_g - T_1). \quad (1)$$

Where:

T_g is the gas flow temperature;

T_1 is the inner surface temperature of the combustion chamber wall;

α is heat transfer coefficient;

$$\alpha = \alpha_T + \alpha_B, \quad (2)$$

α_T is convection heat transfer coefficient;

α_B is radiant heat transfer coefficient.

- **The convection heat transfer coefficient α_T [13]**

The equation for determining the convection heat transfer coefficient is as follows:

$$\alpha_T = K_T \left[kg \left(\frac{2}{k+1}\right)^{\frac{k+1}{k-1}} \right]^{0.4} \frac{p^{0.8}}{(RT_g)^{0.4}} \frac{1}{\overline{D}^{0.2} F^{0.2}}. \quad (3)$$

Where:

$$K_T = \frac{0.023}{g^{0.8}} \frac{\lambda}{\mu^{0.8}} \left(\frac{\upsilon C_P}{\lambda}\right)^{0.4}; \quad (4)$$

$$\overline{D} = \frac{4}{\Pi}. \quad (5)$$

F is the area of cross-section of the combustion chamber; Π is the circumference of the combustion chamber; λ is thermal conductivity coefficient; υ is kinematic viscosity; C_p is Specific heat of combustion gas; g is gravity acceleration; k is the Adiabatic exponent; R is the Thermodynamic constant of gas; T_g is the combustion gas temperature; μ is the density of the combustion chamber material.

- **Radiant heat transfer coefficient α_B [13]**

The combustion product of propellant can be considered to consist of two main components: water vapor and gas. The equation for determining the optical density of a gas according to the thickness of the gas layer is as follows:

$$\varepsilon_\lambda = 1 - e^{-k_B pS}. \quad (6)$$

Where:

k_B is the attenuation coefficient of radiation;

S is the actual thickness of the radiation zone.

Equation (6) shows that the optical density of a gas depends on two different parameters p and S. The radiation occurs mainly from two components: CO_2 and H_2O. The combined optical density of the above two gases is expressed:

$$\varepsilon_r = 1 - e^{-K_r pS}. \quad (7)$$

Where:

$$K_r = \left(\frac{0.78 + 1.6 p_{H_2O}}{\sqrt{(p_{H_2O} + p_{CO_2})S}} - 0.1 \right) \left(1 - 0.37 \frac{T_g}{1000}\right). \quad (8)$$

The radiant heat flow into the engine wall is calculated by the equation:

$$q_B = \varepsilon_r \frac{\varepsilon_T + 1}{2} 4.96 \left[\left(\frac{T_g}{100}\right)^4 - \left(\frac{T_1}{100}\right)^4 \right]. \quad (9)$$

Where:

ε_r is the optical density of nozzle material;

ε_T is the optical density of the gas mixture.

The radiant heat transfer coefficient is calculated as follows:

$$\alpha_B = \varepsilon_r \frac{\varepsilon_T + 1}{2} 4.96 \cdot 10^{-8} {T_g}^3 \frac{1 - \left(\frac{T_1}{T_g}\right)^4}{1 - \left(\frac{T_1}{T_g}\right)}. \quad (10)$$

Considering $\left(\frac{T_1}{T_g}\right)^4 << 1$. equation (10) can be rewritten:

$$\alpha_B = 4.96 \cdot 10^{-8} \varepsilon_r \frac{\varepsilon_T + 1}{2} \frac{{T_g}^3}{1 - \left(\frac{T_1}{T_g}\right)}. \quad (11)$$

The heat loss coefficient in the engine wall:

$$\alpha = 4.96 \cdot 10^{-8} \varepsilon_r \frac{\varepsilon_T + 1}{2} \frac{{T_g}^3}{1 - \left(\frac{T_1}{T_g}\right)} + K_T \left[kg \left(\frac{2}{k+1}\right)^{\frac{k+1}{k-1}} \right]^{0.4} \frac{p^{0.8}}{(RT_g)^{0.4}} \frac{1}{\overline{D}^{0.2} F^{0.2}}. \quad (12)$$

3.1.2 Equation of heat conduction through the engine wall

From the general shape of the rocket engine components, we can assume that the parts are cylindrical tubes. The system of differential equations for heat conduction through the motor wall is the system of differential equations for the heat conduction of a cylinder tube [13,14]. With a thermal protection layer, the heat transfer equation is written as follows:

$$\frac{1}{r^2} \frac{\partial}{\partial r} \left(r^2 \frac{\partial T}{\partial r} \right) + \frac{\dot{E}_{gen}}{k} = \frac{1}{\alpha} \frac{\partial T}{\partial t}. \quad (13)$$

The first condition: $T[0] = T_1$; $r[0] = r_1$.

The boundary conditions:

- At the inner surface:

$$\alpha(T_g - T_1) = -\lambda_1 \left(\frac{\partial t}{\partial n}\right), \quad (14)$$

- At the point of contact of two surfaces:

$$-\lambda_1 \frac{dT_1(r,t)}{dr} = -\lambda_2 \frac{dT_2(r,t)}{dr}, \quad (15)$$

- At the outer surface:

$$\alpha_e(T_3 - T_e) = -\lambda_2 \left(\frac{\partial t}{\partial n}\right). \quad (16)$$

Where:

T_e - environment temperature.

3.2 Establishing the internal ballistic differential equations with the heat loss

3.2.1 Equation for determination of combustion gas temperature with heat loss

For the calculation of powder gas temperature the equation energy balance is used:

$$\frac{d\dot{E}}{dt} = \frac{dU}{dt} + p\frac{dW}{dt} + \frac{dq_l}{dt}. \quad (17)$$

Where:

$\frac{d\dot{E}}{dt} = Q_w.G_{pr}$ is the energy input from powder combustion;

$\frac{dq_l}{dt} = K_q\frac{dq}{dt}$ is heat losses;

$$K_q = \frac{q_l}{c_v T_1 \omega}. \quad (18)$$

$G_{pr} = \frac{d\omega_g}{dt} = \omega\frac{d\psi}{dt}$ is the throughput weight of gas generation during propellant burning;

$Q_w = c_v T_1$ is powder energy content;

c_v is powder isochoric heat capacity;

$\frac{dU}{dt} = c_v\frac{dT_g}{dt}$ is a variation of powder internal energy;

$\frac{dW}{dt} = \left(\frac{\omega}{\delta} - \alpha\omega\right)\frac{d\psi}{dt}$ is a variation of combustion chamber volume during powder burning.

After the substitution of all components in (17), we can get the equation for the calculation of the current gas mixture temperature:

$$\frac{dT_k}{dt} = \frac{G_{pr}}{\omega}\left[T_1\left(1 - K_q\right) - T_k\right]\left(\frac{1}{\delta} - \alpha\right)\frac{\theta}{R}p. \quad (19)$$

Equation of gas generation rate:

$$\frac{d\psi}{dt} = \frac{\rho_T SU}{\omega}. \quad (20)$$

The equation to determine the law of change of combustion chamber pressure:

$$\frac{dp}{dt} = -\frac{1}{V}\left[\left(\phi_2 K_{o(k)} F_{th}\sqrt{f_o} + SU - V\right)p - SUf_o\rho_T\right] \quad (21)$$

The equation for determining the thrust of a solid-propellant rocket engine [15]:

$$P = C_P A_t p. \quad (22)$$

Where: C_p is the thrust coefficient of the rocket engine;

A_t is the throat cross-sectional area of the nozzle.

The total impulse of the thrust is determined by the following equation [15]:

$$I = \int_0^t P dt. \quad (23)$$

The system of interior ballistic equations with heat loss is established when combining equations (13), (17), (19), (20), and (21) as follows.

$$\begin{cases} \frac{dp}{dt} = -\frac{1}{V}\left[\left(\phi_2 K_{o(k)} F_{th}\sqrt{f_o} + SU - V\right)p - SUf_o\rho_T\right] \\ \frac{d\psi}{dt} = \frac{\rho_T SU}{\omega} \\ \frac{dT_k}{dt} = \frac{G_{pr}}{\omega}\left[T_1\left(1 - K_q\right) - T_k\right]\left(\frac{1}{\delta} - \alpha\right)\frac{\theta}{R}\cdot p \\ \frac{d\dot{E}}{dt} = \frac{dU}{dt} + p\frac{dW}{dt} + \frac{dq_l}{dt} \\ \frac{1}{r^2}\frac{\partial}{\partial r}\left(r^2\frac{\partial T}{\partial r}\right) + \frac{\dot{E}_{gen}}{k} = \frac{1}{\alpha}\frac{\partial T}{\partial t} \end{cases} \quad (24)$$

3.3 Establishing the equation for determining the thickness of the thermal protective coating

The thickness of the combustion chamber is determined according to the theory of durability of the thin tube and is only affected by the calculated pressure. The stable condition of the combustion chamber casing is:

$$\Delta_K \geq \frac{1}{2}D_H\left(1 - \frac{[\sigma]}{[\sigma] + p_{tt}}\right). \quad (25)$$

Where:

$[\sigma]$ is the admissible stress of the combustion chamber casing material;

D_H is the internal diameter of the combustion chamber;

p_{tt} is the working pressure of the rocket engine.

The value Δ_K is chosen to suit production technology requirements.

To determine the relationship between the insulation coating thickness and the combustion chamber casing thickness, the Fourier standard is calculated for the coating, and the composition standard is used. This relationship is represented by the following equation [16]:

$$lg\,\theta = lg\,\theta_0 - \frac{A}{\mu + C}Fo. \quad (26)$$

Where:

A, C, and θ_0 are experimental coefficients;

$\theta = \frac{T_g - T_s}{T_g - T_e}$ is the relative temperature;

$$Fo = \frac{a_P t}{\Delta_P^2}, \quad (27)$$

$$\mu = \frac{1}{Bi} + \frac{1}{M} + \frac{1}{Bi \cdot M}, \quad (28)$$

$Bi = \frac{\alpha\Delta_P}{\lambda_1}$ is Biot standard for coatings;

$$M = \frac{\gamma_P c_P \Delta_P}{\gamma_K c_K \Delta_K}; \; a_p = \frac{\lambda_1}{\gamma_P c_P}. \quad (29)$$

- Substituting (27) and (28) into (26), the thickness of the thermal protective coating is determined according to the structural parameters of the combustion chamber and the coating material as follows:

$$\Delta_P = -\frac{1}{2C}\left(\frac{\lambda_1}{\alpha}+\frac{1}{\bar{M}}\right) + \sqrt{\frac{1}{4C^2}\left(\frac{\lambda_1}{\alpha}+\frac{1}{\bar{M}}\right)^2 - \frac{1}{C}\left(\frac{\lambda_1}{\alpha\bar{M}}+\frac{Aa_P\cdot t}{lg\,\theta - lg\,\theta_0}\right)}, \quad (30)$$

$$\bar{M} = \frac{\gamma_P c_P}{\gamma_K c_K \Delta_K}. \quad (31)$$

Where:

t is the working time of the rocket engine;

γ_K, c_K, γ_P, and c_P are the specific weight and specific heat of the combustion chamber wall material and the thermal protection material, respectively; α is the coefficient of heat transfer from the combustible gas to the coating [16].

4. RESULTS AND DISCUSSION

4.1 Input data

The flight engine of the 9M39 rocket is a small rocket engine but has a relatively long working time (~7,2 s). So, the degree of heat loss of this engine during working is relatively large. The components of the 9M39 missile are shown in Fig. 3.

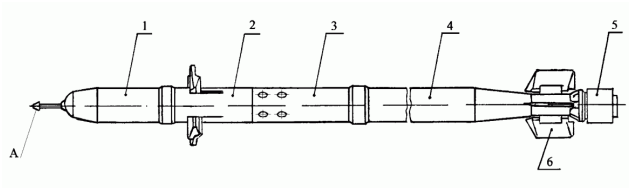

Fig. 3. Components of 9M39 rocket
(1. Infrared seeker; 2. Control section; 3. Warhead; 4. Flight motor; 5. Eject motor; 6. Stabilizers)

To accurately assess the reliability of the theoretical basis established in item 2, the 9M39 rocket flight engine was selected as a model to calculate the thermal protection coating and to evaluate the effect of the thermal protection coating on the performance of solid propellant rocket engines. The input parameters to solve the interior ballistics problem and determine the thickness of the thermal protective coating are shown in Table 1.

The system of differential equations (24) is solved by Matlab software using the initial conditions: $p[1] = p_0$; $\psi[1] = \psi_0$; $q[1] = 0$; $T_k[1]=0$.

The results of solving the problem of interior ballistics with the heat loss of 9M39 missiles are shown in Figs. 4 and 5.

Table 1. Interior ballistic specifications of the 9M39 rocket [17-25]

Parameters	Units	Value
Parameters of combustion chamber material (45X alloy steel)		
Specific weight of	kg/m^3	7820
Specific heat	$kJ/kg\cdot K$	0.5866
Heat conductivity coefficient	$\frac{kJ}{msK}$	$46.5\cdot10^{-3}$
Parameters of thermal protection coating material		
Specific weight	$kg/m^3\,k$	4400
Specific heat	$kJ/kg\cdot K$	0.7039
Heat conductivity coefficient	$\frac{kJ}{msK}$	$0.7027\cdot10^{-3}$
Parameters of interior ballistic problem		
Combustion gas temperature	K	2500
The inner diameter of the combustion chamber	m	$64.5\cdot10^{-3}$
The throat-sectional diameter of the nozzle	m	$14.5\cdot10^{-3}$
Number of nozzles		1
Length of cylindrical part propellant	m	$729.6\cdot10^{-3}$
Length of cone-shaped propellant	m	$95.3\cdot10^{-3}$
Half of the cone angle of the propellant	-	9^o
Diameter of cylindrical part propellant	m	$65.4\cdot10^{-3}$
Minimum diameter of cone-shaped propellant	m	$35.2\cdot10^{-3}$
Density of propellant	kg/m^3	1600
Powder force	J/kg	850000
Adiabatic exponent		1.25
Combustion rate coefficient	$m/s\cdot Pa$	$0.2688\cdot10^{-6}$
Exponential index	-	0.70
Flow loss coefficient	-	0.98

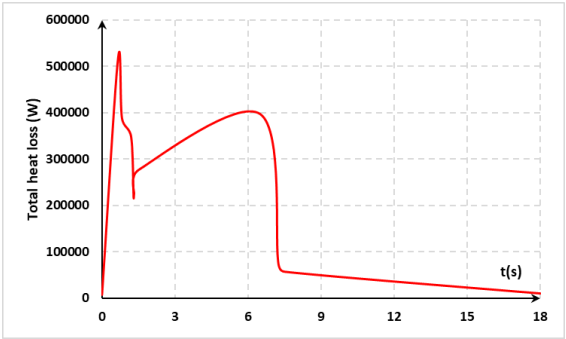

Fig. 4. Graph of heat loss total over time

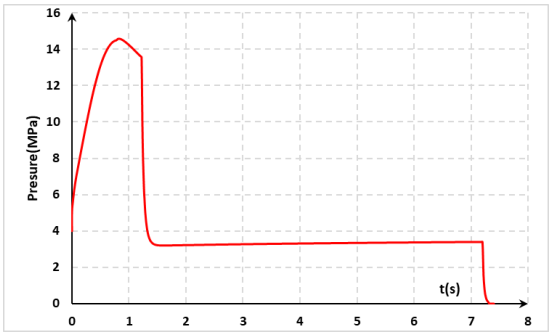

Fig. 5. Graph of combustion chamber pressure over time

4.2 Determination of the thickness of the thermal protective coating for the flight engine of the 9M39 rocket

To evaluate the optimization of the engine mass when calculating the coating thickness, the quantity of mass per square meter of combustion chamber casing $\boldsymbol{M_1 = \gamma_P \Delta_P + \gamma_K \Delta_K}$ is used for comparison. In addition, the allowable stress of the combustion chamber wall material σ_B is also calculated according to the permissible surface temperature T_{CP}. T_{CP} is the maximum temperature of the inner surface at which the material of the combustion chamber wall does not change mechanical properties. The calculation results are shown in Table 2.

Table 2. Table of coating thickness calculation results [26-30]

Parameter analysis	With a thermal protective coating					Without the thermal protective coating
$T_{CP}[^oC]$	300	400	500	550	600	720
$\sigma_B\ [Pa]$	8500	8000	7500	7200	6500	2700
$\Delta_K \cdot 10^{-3}[\ m]$	2.65	2.81	3.00	3.13	3.46	8.33
$\Delta_P \cdot 10^{-3}[m]$	1.83	1.37	1.04	0.89	0.72	0
$M_1\ \left[\frac{kg}{m^2}\right]$	28.79	28.03	28.02	28.38	30.25	65.67

The results of Table 2 show:

- When the allowable temperature T_{CP} is increased, the thickness of the casing of the combustion chamber must be increased.
- The results also show that the engine casing with a thickness of Δ_K= 3mm, a thermal protective coating with a thickness of Δ_P=1.04mm, the mass per square meter of the engine is the smallest $M_1\ \left[\frac{kg}{m^2}\right]$=28.02.
- Compared with the actual parameters of the 9M39 engine, Δ_K= 2.86mm, Δ_P= 1.10mm [11,29, 30], the value of the combustion chamber casing thickness and the thermal protection coating thickness are calculated relatively reliably, the error is within allowable limits, 4.8% and 5.77%, respectively.

If the motor does not have a thermal protective coating, the casing material shall be selected so that the permissible surface temperature is high. Moreover, the thickness of the motor casing must be larger. Thereby increasing the mass of the engine.

4.3 Investigate the effect of thermal protective coating on the thrust of the 9M39 rocket engine

To evaluate the influence of the coating on the thrust of the engine, the thrust of the engine is calculated in 2 cases:

- Engine with thermal protection coating;
- Engine without thermal protection coating.

The results of solving the system of differential equations (24) combined with the equations of thrust (22), and impulse (23), the law of temperature of the inner surface of the combustion chamber wall T_2, thrust of the engine, and impulse *I* for 2 cases are determined as shown in Figs. 6, 7 and Table 3.

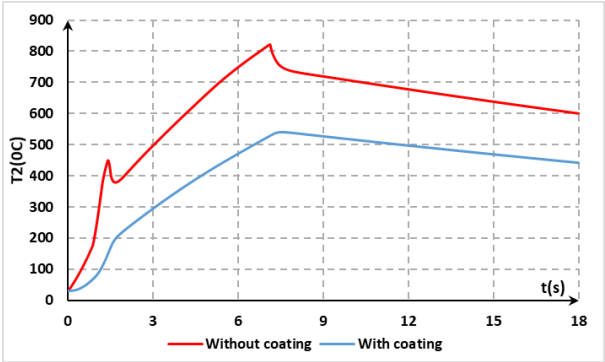

Fig. 6. Graph of inner surface temperature in the combustion chamber wall over time

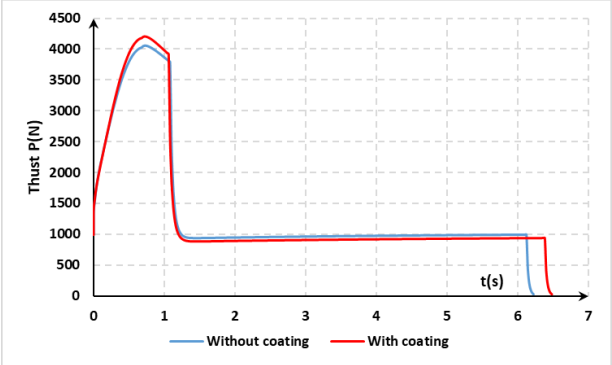

Fig. 7. Graph of thrust corresponding to the time

Figs. 6, 7 and Table 3 show:

- With a thermal protective coating applied, the internal surface temperature of the combustion chamber wall is significantly reduced (from 820^0C to 540^oC). With this surface temperature, the engine can work for a longer time while the combustion chamber casing is not destroyed.

- Thrust is also lost to less heat in the presence of a thermal protective coating. Specifically, maximum thrust decreased by 1.42%, cruise thrust decreased by 1.04% and total impulse decreased by 1.13%.

Table 3. The thrust and total impulse

Parameter analysis	P_{max} (N)	P_{ht} (N)	I (N·s)
With coating	4126	1019	10068
Without coating	4068	979	8902
Difference (%)	1.42	1.04	1.13

5. CONCLUSION

In the content of this paper, the model used to calculate the thickness of the thermal protective coating is presented, and the relationship between the thickness of the thermal protective coating and the thickness of the combustion chamber casing is specifically established. Based on the simulation results, the following conclusions can be drawn.

(1) The selection of thermal protection materials for rocket engines must meet the following requirements: Light density, small coefficient of thermal conductivity, good wear resistance, and ease of fabrication.

(2) The combustion gas temperature is very high, greatly affecting the mechanical properties of the combustion chamber shell material, which distorts the structural parameters of the engine, and the accuracy of the control signal is reduced. Therefore, rocket engines with long work time and guided rocket engines necessarily have thermal protective coatings.

(3) The research results of the article are a reliable theoretical basis for calculating the thermal protection coating thickness for similar types of solid-fuel rocket engines, especially anti-aircraft missiles, anti-tank missiles, cruise missiles, etc, which have a relatively long working time.

The limitations of this model are directly related to the simplifying hypotheses used. However, the method can be utilized to determine selection criteria for new insulation materials or to guide the designer in choosing between available materials.

ACKNOWLEDGEMENT

This research is funded by Le Quy Don Technical University Research Fund under the grand number "23.1.23".

REFERENCES

[1] T.A. Man'ko, K.V. Kozis, The Issues of Chemistry and Technologies of Resin Mixtures Fabrication for Internal Heat-Protective Coating of Rocket Solid Fuel Engine. *Journal of Rocket - Space Technology*, 27(4), 2019: 13-20. https://doi.org/10.15421/451903

[2] M.G. Domingues, J.A.F.F, Rocco, High-temperature coating: hybrid rocket motor thermal protection case history. *International Journal of Energetic Materials and Chemical Propulsion*, 16(2), 2017: 165-174.

[3] L.F.S. Hoffmann, F.C.P. Bizarria, J.W.P, Bizarria, Applied algorithm in the liner inspection of solid rocket motors. *Optics and Lasers in Engineering*, 102, 2018: 143-153. https://doi.org/10.1016/j.optlaseng.2017.11.006

[4] R. Duval, A. Soufiani, J. Taine, Coupled Radiation and Turbulent Multiphase Flow in an Aluminised Solid Propellant Rocket Engine. *Journal of Quantitative Spectroscopy & Radiative Transfer*, 84(4), 2004: 513-526. https://doi.org/10.1016/S0022-4073(03)00268-1

[5] D. Lemić, Geometrical influence on solid rocket propellant ignition. *Scientific Technical Review*, 56(3-4), 2006: 12-20.

[6] J.Y. Jung, M.Q. Brewster, Radiative Heat Transfer Analysis with Molten Al2O3 Dispersion in Solid Rocket Motors. *Journal of Spacecraft and Rockets*, 45(5), 2008: 1021-1030. https://doi.org/10.2514/1.30018

[7] Q. Ye, Y.-g. Yu, G., W.-f. Li, Study on cook-off behavior of HTPE propellant in solid rocket motor. *Applied Thermal Engineering*, 167 2020: 114798. https://doi.org/10.1016/j.applthermaleng.2019.114798

[8] V.T. Nguyen, D.S. Nguyen, External Ballistic Textbook. *Military Technical Academy*, Hanoi 2003. p.379. (in Vietnamese)

[9] R.C. Farmer, S.D. Smith, B.L. Myruski, *Radiation from Advanced Solid Rocket Motor Plumes*. *NASA*, NASA CR-196554 Final Report, 1994.

[10] D.V. Doan, V.V. Bien, M.A. Quang, N.M. Phu, A study on multi-body modeling and vibration

analysis for twin-barrel gun while firing on elastic ground. *Applied Engineering Letters*, 8(1), 2023, 36-43. https://doi.org/10.18485/aeletters.2023.8.1.5

[11] T.N. Hai, T.N. Dung, Equipment with jet weapons. *Military Technical Academy*, Hanoi, 2016. (in Vietnamese).

[12] S.W. Baek, M.Y. Kim, *Analysis of Radiative Heating of a Rocket Plume Base with the Finite-Volume Method*. *International Journal of Heat and Mass Transfer*, 40(7), 1997: 1501-1508. https://doi.org/10.1016/S0017-9310(96)00257-8

[13] Q. Wu, J. Liu, Y. Jin, Y. Chen, L. Du, L.M. Waqas, Thickness measurement method for the thermal protection layer of a solid rocket motor based on a laser point cloud. *Insight-Non-Destructive Testing and Condition Monitoring*, 64(4), 219-228: 2022. https://doi.org/10.1784/insi.2022.64.4.219

[14] T.S. Ngo, S. Beer, V.V. Bien, P.D. Nguyen, P.M. Nguyen. Oscillation of the Anti-tank missile system Fagot fired on the Elastic ground. *2019 International Conference on Military Technologies (ICMT)*, 30-31 May 2019, Brno, Czech Republic. https://doi.org/10.1109/MILTECHS.2019.8870069

[15] A.M. Enew, A.M. Elfattah, S.R. Fouda, S.A. Hawash, Effect of aramid and carbon fibers with nano carbon particles on the mechanical properties of EPDM rubber thermal insulators for solid rocket motors application. *Polymer Testing*, 103, 2021: 107341. https://doi.org/10.1016/j.polymertesting.2021.107341

[16] A. Turchi, D. Bianchi, P. Thakre, F. Nasuti, V. Yang, Radiation and Roughness Effects on Nozzle Thermochemical Erosion in Solid Rocket Motors. *Journal of Propulsion and Power*, 30(2) 2014:314-324. https://doi.org/10.2514/1.B34997

[17] D. Bianchi, A. Neri, Numerical Simulation of Chemical Erosion in Vega Solid-Rocket-Motor Nozzles, *Journal of Propulsion and Power*, 34(2), 2018: 482–498. https://doi.org/10.2514/1.B36388

[18] T.H. Nguyen, M.P. Nguyen, Vibration of launcher on multiple launch rocket system BM-21 with the change of rocket's mass center when fired. *Journal of Science and Technique*, 14(03), 2019. https://doi.org/10.56651/lqdtu.jst.v14.n03.443

[19] H.T. Martin, A.C. Cortopassi, K.K. Kuo, Assessment of the Performance of Ablative Insulators Under Realistic Solid Rocket Motor Operating Conditions. *International Journal of Energetic Materials and Chemical Propulsion*, 16(1), 2017: 1-22.

[20] Parry, D. L., and Brewster, M. Q., Optical Constants of Al2O3 Smoke in Propellant Flames. *Journal of Thermophysics and Heat Transfer*, 5(2), 1991: 142-149. https://doi.org/10.2514/3.241

[21] P.G. Cross, I.D. Boyd, Reduced Reaction Mechanism for Rocket Nozzle Ablation Simulations. *Journal of Thermophysics and Heat Transfer*, 32(2), 2018: 429-439. https://doi.org/10.2514/1.T5291

[22] M.P. Nguyen, T.H. Nguyen, V.B. Vo, Contour design for solid propellant rocket-engine nozzle. *Journal of Science and Technology*, 15(01), 2020: 13-22. https://doi.org/10.56651/lqdtu.jst.v15.n01.105

[23] F. Krejčíř, P. Konečný, PG-7V Ammunition as an Indirect Fire Threat, *2019 International Conference on Military Technologies (ICMT)*, 30-31 May 2019, Brno, Czech Republic, pp.1-4. https://doi.org/10.1109/MILTECHS.2019.8870046

[24] D.P. Nguyen, M.P. Nguyen, B.T. Phan, V.B. Vo, T.H. Nguyen, Study on the Influence of Some Structural Features of the Stabilizer Fins on the Stability of Unguided Rockets. *2023 International Conference on Military Technologies (ICMT),* 23-26 May 2023, Brno, Czech Republic. https://doi.org/10.1109/ICMT58149.2023.10171280

[25] D.P. Nguyen, Researching the Effects of Some Initial Disturbance Factors on Firing Accuracy, PhD Thesis. *Military Technical Academy*, Hanoi, 2016. p.134. (in Vietnamese)

[26] H.B. Le, Konečný, P. Effect of Some Disturbance Factors on the Motion Stability of Unguided Rockets. *Advances in Military Technology*, 15(2), 2020: 405-423. https://doi.org/10.3849/aimt.01379

[27] E. Cavallini, F. Bernardo, A. Neri, Analysis and performance reconstruction of VEGA solid rocket motors qualification flights. *50th AIAA/ASME/SAE/ASEE Joint Propulsion Conference*, 28-30 July, 2014, Cleveland, USA. https://doi.org/10.2514/6.2014-3805

[28] T.H. Nguyen B.V. Vo, Evaluation of the effect of the thrust deviation on the BM-21 launcher's

oscillation in a single volley. *Journal of Science and Technology*, 2016.

[29] P. Koněčný, Z. Křižan, Determination of black powder burning rate. *Advances in Military Technology,* 3(2), 2008, 11-18.

[30] F. Krejčíř, R. Buldra P. Konečný, Ignition of Small Rocket Motor Using Black Powder Igniters. *2021 International Conference on Military Technologies (ICMT),* 8-11 June 2021, Brno, Czech Republic, pp.1-8. https://doi.org/10.1109/ICMT52455.2021.9502780